

The A_y -Problem in Refined Resonating Group Model calculations for $(p - {}^3\text{He})$ Scattering

C. Reiß^{a,b} and H.M. Hofmann^a

^a *Institut für Theoretische Physik III, Universität Erlangen-Nürnberg,
Staudtstraße 7, D-91058 Erlangen, Germany*

^b *Department of Physics and Astronomy, University of Victoria, 3800 Finnerty
Rd., Elliot Bldg., Victoria, BC V8P 1A1, Canada*

Abstract

We report on a microscopic Refined Resonating Group Model (RRGM) calculation of scattering of p off ${}^3\text{He}$ employing the Argonne- v_{14} and the Bonn nucleon-nucleon potentials without three-nucleon forces at low energies up to 30 MeV. The calculated phase-shifts verify the well-known proton analyzing power A_y -problem. We demonstrate that with corrected 3P_2 phase-shifts experimental differential cross-section and analyzing power data can be explained.

Key words: phase-shift, analyzing power, Refined Resonating Group Model, realistic NN -interactions

PACS: 21.45.+v, 24.70.+s, 25.40.Cm

1 Introduction

It is widely known that realistic nucleon-nucleon (NN) forces cannot reproduce the ${}^3\text{H}$ and ${}^3\text{He}$ binding energies. The A_y analyzing power in $(N - d)$ scattering is still not reproduced by adding three-nucleon interactions [1]. The 30% deviation of A_y can be resolved by tiny changes on the order of 0.1° in the $(N - d)$ scattering phase-shifts [2,3,4]. It was shown in [5] that although a realistic NN -force can generally reproduce the ${}^4\text{He}$ system, there remain differences, most notably in the analyzing powers. Recently Fonseca et al. [6] studied the $(n - {}^3\text{He})$ scattering system using an AGS-approach. They calculated the cross-sections and vector analyzing powers using the NN -interactions Bonn-CD [7], Nijmegen II [8] and Bonn-B [9] without $3N$ -forces

Email address: reissc@kph.uni-mainz.de (C. Reiß).

and pointed out that the $(n - {}^3\text{He})$ system may turn into a A_y puzzle like it is known in $(n - d)$ scattering and may be cured by $3N$ -forces. The detailed studied ${}^4\text{He}$ system [10] is unfortunately extremely difficult to describe due to the ${}^4\text{He}$ bound-state and particularly the complex resonance-structure. For that reason we investigate the much simpler system $(p - {}^3\text{He})$, the ${}^4\text{Li}$. In the studied energy range up to 30 MeV is a lot of data available. And we have restricted ourselves on realistic NN -interactions without three particle forces namely the Argonne- v_{14} -potential [11] and the Bonn-potential in the form of Ref. [12].

The paper is organized as follows: In section 2 we give a brief introduction to the RRGM. We present in section 3 for each of the interactions (Argonne- v_{14} and Bonn) two model-spaces (a medium and large one) for the used RRGM scattering calculation. Then we compare and discuss in section 4 the obtained phase-shifts δ , analyzing powers A_y and differential cross-section $d\sigma/d\Omega_{\text{c.m.}}$ with experimental data and demonstrate the origin of the A_y -problem.

2 Refined Resonating Group Model with Distortion channels

2.1 Refined Resonating Group Model

This calculation is based on the Refined Resonating Group Model (RRGM) [13] with distortion channels [14]. Therefore we briefly summarize the RRGM in the following.

The model employed is restricted to a two fragment description. That means the model is not able to describe the three particle breakup reactions. Therefore a scattering channel consists of two fragments $i = 1, 2$ with total angular momentum J_i which couple to the channel spin S_c . The channel spin S_c couples with the relative orbital angular momentum L_{rel} to the total angular momentum J of the channel ${}^{2S_c+1}L_{\text{rel},J}$. The binding energy and the wavefunction of one fragment is obtained using the variational principle of Ritz. The solution of the Schrödinger-Equation for the scattering problem is won by the variational principle of Kohn-Hulthén [15].

The Hamilton-operator H for a N -particle system with a two-body-force is given by:

$$H(1, \dots, N) = \sum_{i=1}^N T_i + \sum_{\substack{i,j=1 \\ i < j}}^N V_{ij} \quad . \quad (1)$$

Using momentum conservation, the center-of-mass energy $T_{\text{c.m.}}$ is separated off. The restriction to a two-fragment model allows to formulate a translation-

ally invariant Hamilton-operator H' consisting of fragment and relative-motion parts. The potential term becomes shortranged by subtracting the Coulomb-potential $Z_1 Z_2 e^2 / R$ with the relative coordinate \mathbf{R} between the fragments:

$$H'(1, \dots, N) = H_1(1, \dots, N_1) + H_2(N_1 + 1, \dots, N) + T_{\text{rel}} + Z_1 Z_2 e^2 / R + \left(\sum_{\substack{i \in \{1, \dots, N_1\} \\ j \in \{N_1 + 1, \dots, N\}}} V_{ij} - Z_1 Z_2 e^2 / R \right) . \quad (2)$$

With the variational principle of Kohn–Hulthén [15]

$$\delta \left(\langle \Psi_l | H' - E | \Psi_l \rangle - \frac{1}{2} a_{ll} \right) = 0 \quad (3)$$

we determine the solution of the Schrödinger-Equation where the scattering wavefunction is denoted by Ψ_l . From the reaction matrix a the scattering matrix S is calculated via the Cayley–Transformation:

$$S = (\mathbb{1} + ia) (\mathbb{1} - ia)^{-1} . \quad (4)$$

The index l in Eq.(3) is the label of the corresponding boundary condition. The ansatz for the wavefunction Ψ_l is

$$\Psi_l = \mathcal{A} \left\{ \sum_{k=1}^{n_k} \Psi_c^k \cdot \Psi_{\text{rel}}^{lk} \right\} , \quad (5)$$

with the antisymmetrization operator

$$\mathcal{A} = \sum_P (-1)^P P \quad (6)$$

where P is the permutation over all particles, n_k is the number of channels, Ψ_c^l is the channel function and Ψ_{rel}^{lk} is the relative wavefunction:

$$\Psi_{\text{rel}}^{lk}(R) = \delta_{kl} F_k(R) + a_{lk} \tilde{G}_k(R) + \sum_m b_{lkm} \chi_{km}(R) . \quad (7)$$

F_k and \tilde{G}_k are regular and regularized irregular Coulomb-functions for the correct description of the asymptotic behavior of the wavefunction. δ_{kl} is here the Kronecker-Symbol. The χ_{km} are square-integrable functions for the description of the wavefunction in the interaction region. The variation of the a_{lk} and the b_{lkm} yields with Eq.(4) the S -Matrix:

$$S_{kl} = \eta_{kl} e^{2i\delta_{kl}} \quad (8)$$

with phase-shifts δ_{kl} and channel coupling-strengths η_{kl} .

The scattering wavefunction Ψ_l (see Eq.(5)) was already explained but without the channel part. We look only at one term in Eq.(5). It is convenient to make the following ansatz for the channel function Ψ_c :

$$\Psi_c = \left[\frac{Y_{L_{\text{rel}}}(\hat{\mathbf{r}})}{r} \otimes [\phi_1^{J_1} \otimes \phi_2^{J_2}]^{S_c} \right]^J. \quad (9)$$

We use $\phi_i^{J_i}$ ($i = 1, 2$) for the translational invariant wavefunction of the i th fragment with spin J_i . In Eq.(9) square brackets indicate the angular momentum coupling. In the case of scattering calculation the coordinate \mathbf{r} is the relative coordinate \mathbf{R} . If $\Psi_{\text{rel}}(\mathbf{r})$ is a bound-state wavefunction then there will be no coupling to the channel spin S_c and the coordinate \mathbf{r} will be the Jacobi-coordinate between the center-of-mass of the both fragments. The fragment function ϕ^J is build of the spin-isospin function Ξ and of the spatial function χ :

$$\phi^J = \sum_{l_I, S, \alpha} [C_\alpha^{l_I L S} \chi_\alpha^{l_I} \Xi^{ST}] \quad (10)$$

The set of inner orbital angular momenta in the fragments is labeled with l_I . The corresponding fragment consists of n nucleons. The spin-isospin functions Ξ are coupled to good total spin and good isospin. The Clebsch-Gordan-coefficients of the coupling of the orbital angular momenta l_1, l_2, \dots, l_{n-1} to the total orbital angular momentum L , the coefficients of the coupling of the spins and isospin are coupled to S and T and the coefficients of the super-position of the radial dependencies α are expressed by the factor $C_\alpha^{l_I L S}$. The $\chi_\alpha^{l_I}$ are the square-integrable spatial functions. They consist of nucleon relative functions $\chi_{\alpha, k}^{l_k}$:

$$\chi_\alpha^{l_I} = \prod_{k=1}^{n-1} \chi_{\alpha, k}^{l_k} \quad (11)$$

The nucleon relative function consists from a Gaussian function with width parameter $\beta_{\alpha, k}$ and from a Solid-Spherical-Harmonics \mathcal{Y} [16]:

$$\chi_{\alpha, k}^{l_k} = \exp \left\{ -\beta_{\alpha, k} \rho_k^2 \right\} \mathcal{Y}_{l_k, m_k}(\boldsymbol{\rho}_k), \quad (12)$$

where $\boldsymbol{\rho}_k$ is the Jacobi-coordinate between the $(k + 1)$ th nucleon and the center-of-mass of the nucleons $(1, 2, \dots, k)$.

All spatial functions are in this model finally parametrized with Gaussian functions.

2.2 Distortion Channels

Distortion channels in the RRGm are unphysical bound-states which can be chosen arbitrarily as far as they are linear independent and as long as they

have right total angular momentum and total parity. They are allowed to violate e.g. the channel spin S_c of the scattering channels. Distortion channels have the asymptotics of bound-state channels. The idea of including distortion channels is to enlarge the model-space in the region of interaction. Therefore distortion channels can be used to describe physical structures which can not be described by the RRGM or are not included in the scattering channels e.g. deformations of the fragments, excited fragments and scattering-states which are not yet opened channels. A more detailed description of the approach using distortion channels with the RRGM can be found by R. Wölke [14].

3 Model-Spaces for $(p - {}^3\text{He})$ Scattering

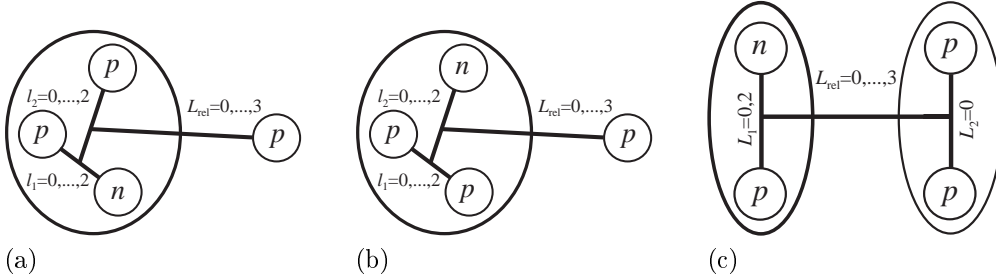


Fig. 1. Panel (a) and (b) show the $(p - {}^3\text{He})$ -structures and subfigure (c) shows the $(d - {}^2\text{He})$ -structure used to describe the $(p - {}^3\text{He})$ -scattering-system with $L_{\text{rel}} \leq 3$.

For the description of the ${}^4\text{Li}$ -scattering-system with $L_{\text{rel}} \leq 3$ and $J^\pi = 0^\pm, 1^\pm, 2^\pm, 3^+$ we have used the sets of Jacobi-coordinates with orbital angular momenta as indicated in Fig.1. We have studied this scattering-system with the Argonne- v_{14} - (av_{14}) and the Bonn-potential. For the ${}^3\text{He}$ -subsystem we have used two different model spaces: a medium system (labeled with HeM) with 5 basis-vectors and a large ${}^3\text{He}$ -subsystem (labeled with HeG) with 23 basis-vectors. The $(p - {}^3\text{He})$ -scattering-system using the large ${}^3\text{He}$ -subsystem was studied without F -wave scattering because the F -wave phase-shifts turned out very small in the medium system $(p - {}^3\text{He})$ -system. Table 1 shows the used model-spaces in compact form. The sets of width parameters consisting of n_1 elements on the first Jacobi-coordinate and n_2 on the second indicated in brackets are assigned to spin-isospin-functions with the choice of angular momenta. The sets of widths are determined by a non-linear optimization [17]. In the scattering calculation for the large ${}^3\text{He}$ -subsystem the smallest width on the second coordinate was dropped due to the fact that there was practically no improvement of the ${}^3\text{He}$ wave-function. For the rearrangement channel $(d - {}^2\text{He})$ we used for the description of the deuteron d three width parameters for the S -wave and two for the D -wave. The unbound ${}^2\text{He}$ -system is described with an S -wave using the S -wave width set of the deuteron. The rearrangement channel $(d - {}^2\text{He})$ opens in the medium system at 5.7 MeV using the

Argonne- v_{14} - and at 6.5 MeV using the Bonn-interaction. For the large model these energies are 7.1 MeV (av_{14}) and 7.6 MeV (Bonn). The binding-energies E_B , the charge r.m.s.-radii and the D -state probabilities of the models are summarized in Tab. 2 and Tab. 3. As expected the D -state probabilities for the Argonne- v_{14} -interaction are appreciably higher than those for the Bonn-potential, see table 3. With increasing the model-space the binding-energy is improved and also the r.m.s.-radii. The r.m.s.-radii are smaller than the experimental ones and they are even smaller for smaller model-spaces. Naturally one would expect for models which underbind the system to generate larger r.m.s.-radii. Here, however, in the smaller model-spaces those width parameters, which generate the larger radii, are missing. A basis-vector of the ^4Li -scattering-system is therefore a spin-isospin function consisting of one neutron and three protons with a fixed orbital angular momentum configuration and the appropriate set of width parameters. The set of distortion channels for both models was obtained by using the $(d - ^2\text{He}^*)$ and $(d - ^2\text{He}^{**})$ channels as distortion-channels because they open at energies higher than 30 MeV and are therefore out of the studied range of energies. In addition as much as possible of the existing basis-vectors have been used to form the maximum of linear independent distortion-channels. Every additional distortion channel contains therefore only one basis-vector. For the scattering-channel the set of widths w_{rel} was used on the relative coordinate, where for the distortion channels only the subset w_{dist} was taken on that coordinate.

4 Results and Discussion

4.1 $(p - ^3\text{He})$ phase-shifts

In this subsection phase-shifts are diagonal-phase-shifts. Published eigen-phase-shifts have been transformed to diagonal-phase-shifts.

Unfortunately there are no modern theoretical phase-shift calculations at higher energies up to $E_{\text{c.m.}} = 30$ MeV. Only Reichstein et al. [21] and Heiss et al. [22] did Resonating Group Model calculations using a much smaller model-space and a much simpler NN -interaction in the considered energy range. Reichstein et al. used a purely central NN -potential. Heiss et al. used a softcore central, spin-orbit and tensor-force potential. Beltramin et al. [23] made a separable potential model up to $E_{\text{c.m.}} = 10$ MeV. We will not compare their results with ours since their models are much simpler than ours. Viviani et al. [24] recently studied the elastic $(p - ^3\text{He})$ -scattering-system using the Kohn variational principle with correlated hyperspherical harmonics. As interaction Viviani et al. used the av_{18} - NN -interaction [25] and the av_{18} - NN -interaction with the Urbana IX $3N$ -potential [26]. Unfortunately they

Model		[[T ₁ T ₂] ^s T ₃]] ^S		(l ₁ l ₂) ^L	
HeM	(3+2)	[[np] ^{0,1} p] ^{1/2}	(00) ⁰		
		[[pp] ⁰ n] ^{1/2}	(00) ⁰		
		[[np] ¹ p] ^{3/2}	(20) ²	(02) ²	
HeG	(3+3)	[[np] ^{0,1} p] ^{1/2}	(00) ⁰	(11) ^{0,1}	
		[[pp] ⁰ n] ^{1/2}	(00) ⁰		
		[[pp] ¹ n] ^{1/2}	(11) ^{0,1}		
		[[Np] ¹ \bar{N}] ^{3/2}	(11) ^{1,2}		
		[[np] ^{0,1} p] ^{1/2}	(22) ^{0,1}		
		[[pp] ⁰ n] ^{1/2}	(22) ^{0,1}		
		[[np] ¹ p] ^{3/2}	(20) ²	(02) ²	(22) ^{1,2}
w _{rel} [fm ⁻²] (20)	12.95665	5.134670	<u>2.947287</u>	1.342339	<u>0.821446</u>
<u>w_{dist} [fm⁻²]</u> (5)	0.444741	<u>0.293900</u>	0.169016	<u>0.118524</u>	0.084300
	<u>0.050011</u>	0.025737	0.013852	0.007143	0.003852
	0.001857	0.000973	0.000562	0.000277	0.000101

Table 1: The model-spaces for the ${}^3\text{He}$ -system is given in the upper two third of the table. The sets of widths are assigned to the spin-isospin-function and angular momentum structures. The number of sets of widths on the first and the second Jacobi-coordinates is indicated in brackets. (N is p or either n and therefore $\bar{N} \neq N$ denotes n or p). The sets of widths for the relative coordinate in the ${}^4\text{Li}$ -scattering-system for the scattering- w_{rel} and distortion-channels w_{dist} (underlined) are given in the lower third of the table.

published only results for very low energies ($E_{\text{c.m.}} \leq 1.69$ MeV). Pfitzinger et al. [27] did an R -matrix analysis and an RRGm calculation but only at low energies ($E_{\text{c.m.}} < 5$ MeV). We will not include the results of Pfitzinger et al. into the figures. In the following we will compare our results with the phase-shift analysis based on experimental data in the desired energy-region of Darves-Blanc et al. [28], McSherry et al. [29], Müller et al. [30] and Tombrello [31].

The phase-shifts obtained by the RRGm calculation using the medium model-space are compared with the results of other groups in Fig. 2-4. The S -wave phase-shifts, shown in figure 2, are in very good agreement in the whole range of interest with the results obtained by others [24,28,29,30,31]. The S -wave

NN -Interaction		Argonne- v_{14}	Bonn
$E_B(d)$	[MeV]	-1.878	-1.911
$E_B^{\max}(d)$	[MeV]	-2.222	-2.222 [12]
$E_B^{\text{exp}}(d)$	[MeV]	-2.225 [18]	
$E_B^M(^3\text{He}^{1/2+})$	[MeV]	-5.588	-6.287
$E_B^G(^3\text{He}^{1/2+})$	[MeV]	-6.895	-7.416
$E_B^{\max}(^3\text{He}^{1/2+})$	[MeV]	-6.949	-7.492
$E_B^{\text{exp}}(^3\text{He}^{1/2+})$	[MeV]	-7.718 [19]	

Table 2: The binding-energies E_B of the used model-spaces for the fragments in the ^4Li -scattering-system are summarized. For comparison the experimental data (exp) and the best result of a RRGm calculation (max) are shown for the different studied NN -interactions Argonne- v_{14} and Bonn.

NN -Interaction		Argonne- v_{14}	Bonn
$r_{\text{r.m.s.}}(d)$	[fm]	1.80 (5.37%)	1.77 (4.51%)
$r_{\text{r.m.s.}}^{\max}(d)$	[fm]	1.98 (6.08%)	1.98 (4.78%)
$r_{\text{r.m.s.}}^{\text{exp}}(d)$	[fm]	2.13 [20]	
$r_{\text{r.m.s.}}^M(^3\text{He}^{1/2+})$	[fm]	1.72 (7.47%)	1.62 (5.93%)
$r_{\text{r.m.s.}}^G(^3\text{He}^{1/2+})$	[fm]	1.86 (8.98%)	1.76 (6.96%)
$r_{\text{r.m.s.}}^{\max}(^3\text{He}^{1/2+})$	[fm]	1.88 (9.00%)	1.78 (7.05%)
$r_{\text{r.m.s.}}^{\text{exp}}(^3\text{He}^{1/2+})$	[fm]	1.97 [19]	

Table 3: The charge r.m.s.-radii $r_{\text{r.m.s.}}$ of the used model-spaces for the fragments in the ^4Li -scattering-system are summarized. For comparison the experimental data (exp) and the best result of a RRGm calculation (max) are shown for the different studied NN -interactions Argonne- v_{14} and Bonn. The D -state probability of each model is shown in parentheses.

phase-shifts are all negative due to the underlying Pauli-forbidden states. The D - and F -wave phase-shifts are not shown because they are small and they are in good agreement with the results of others cited where the D -wave phase-shifts are between -10° and 0° in the whole energy range. The F -wave phase-shifts are even smaller than the D -wave phase-shifts by a factor of

about 10. For the P -wave phase-shifts, see figure 3, however, the situation is different. They are all positive. The RRGm reproduces the over-all behavior quite well, but the maximal values are never reached, that means that all P -wave phase-shifts are not attractive enough. Furthermore the maxima occur at too low energies. The Bonn-interaction reproduces these phase-shifts slightly better. Since the Bonn-potential underbinds the ${}^3\text{He}$ less than the Argonne- v_{14} -interaction (see Tab. 2). Both forces predict also a too small r.m.s.-radius in the studied model-spaces where Argonne-interaction gives a better description (see Tab. 3). Generally the Bonn-interaction yields a slightly better description of the ${}^3\text{He}$ subsystem than the Argonne- v_{14} -force and yields therefore to a slightly better description (see Tab. 2 and Tab. 3).

The analysis of McSherry et al. and Tombrello disagree around 5 MeV for the 1P_1 (Fig. 3 (b)) and 3P_1 (Fig. 3 (c)). From general consideration we consider the results of Tombrello more reliable, as they indicate only a weak j-splitting. Our results for the 1^- phase-shifts are quite similar to those of Pfitzinger et al. [27].

But for the 3P_2 phase-shift analysis (Fig. 3 (d)) the results of the other groups are consistent. Here we have a good reproduction at low energies ≤ 3 MeV. Then our phase-shift shows clearly not enough attraction. Also Pfitzinger et al. [27] reported that they are not able to reproduce the 3P_0 and the 3P_2 phase-shift. Therefore we will concentrate in the following on the 3P_2 phase-shift.

In Fig. 4 we compare the 3P_2 phase-shift calculated using the Bonn-interaction for the medium and the large model-space with the results of others as indicated. It turns out that the better ${}^3\text{He}$ wavefunction does not necessarily lead to a better description of the phase-shift although this model reproduces more accurately the binding-energy and r.m.s.-radius (see Tab. 2 and Tab. 3). Similar results have been obtained using the Argonne- v_{14} -interaction. The overall description of the phase-shifts is improved using the large model-space but the P -wave phase-shifts show less attraction than in the medium model. In the medium model the P -wave phase-shifts drop too fast at higher energies because of the too small r.m.s.-radius in comparison to the larger model-space.

4.2 Analyzing powers A_y and differential cross-section $d\sigma/d\Omega_{\text{c.m.}}$

To check if the 3P_2 phase-shift carries the main contribution of the so-called A_y -problem we will take now a closer look at analyzing-power A_y and the differential cross-section $d\sigma/d\Omega_{\text{c.m.}}$. We compare the analyzing-power A_y and the differential cross-section at $E_{\text{c.m.}} = 5.20$ MeV and at $E_{\text{c.m.}} = 22.5$ MeV with data, namely Birchall et al. [32], McCamis et al. [33], McDonald et al.

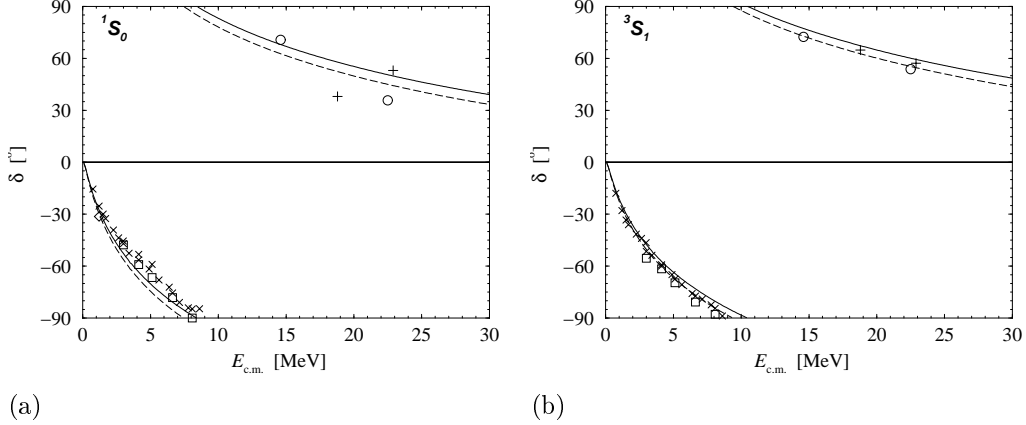


Fig. 2. The 1S_0 (a) and the 3S_1 phase-shifts (b) of $(p - ^3\text{He})$ scattering using the medium model-space for the ^3He wave-function for the Argonne- v_{14} (dashed line) and the Bonn (solid line) interaction in comparison with experimental and theoretical results from other groups is shown: Darves-Blanc et al. [28] (\circ), McSherry et al. [29] (\square), Müller et al. [30] ($+$), Tombrello [31] (\times) and Viviani et al. [24] (\diamond).

[34] and McSherry et al. [29] for the analyzing-power results and McDonald et al. [34] and Harbison et al. [35] for the cross-section results. The error bars are increased in comparison to the original ones of McCamis et al. [33] because we took the values from the their figures since the data was not tabulated.

In Fig. 5 we compare the results for the differential cross-section of McDonald et al. at $E_{\text{c.m.}} = 5.21$ MeV and Harbison et al. at $E_{\text{c.m.}} = 23.0$ MeV with our calculation in the medium Bonn-model at $E_{\text{c.m.}} = 5.20$ MeV (solid line) and $E_{\text{c.m.}} = 22.5$ MeV (dotted dashed line). The curves in Fig. 5 (dashed line and dotted line) correspond to calculations where the 3P_2 phase-shift has been modified. We have added at $E_{\text{c.m.}} = 5.20$ MeV 10.5° and at $E_{\text{c.m.}} = 22.5$ MeV 15.0° to reach the experimental 3P_2 phase-shift in the S -matrix-element. Figure 5 shows that we are now in very good agreement with the experiment at $E_{\text{c.m.}} = 5.20$ MeV. But at $E_{\text{c.m.}} = 22.5$ MeV it turns out that a better description of the 3P_2 phase-shift is not enough to explain the experimental data. At least we get a good agreement for angles above 110° .

Since looking on the differential cross-section can only provide a rough overview of the quality of the calculation because the differential cross-section is not too sensitive to the particle spin. Therefore we study now the much more sensitive analyzing-powers (see Fig. 6). We employed the same modifications as for the differential cross-section, setting the 3P_2 phase-shift to its experimental value. The calculated analyzing-powers A_y demonstrate that 3P_2 phase-shift has the main contribution to the A_y -problem. In fact all P -wave phase-shifts show too less attraction. Including the 3F_2 -channel does not change the results. Therefore the tensor-force has no strong contribution to the A_y problem.

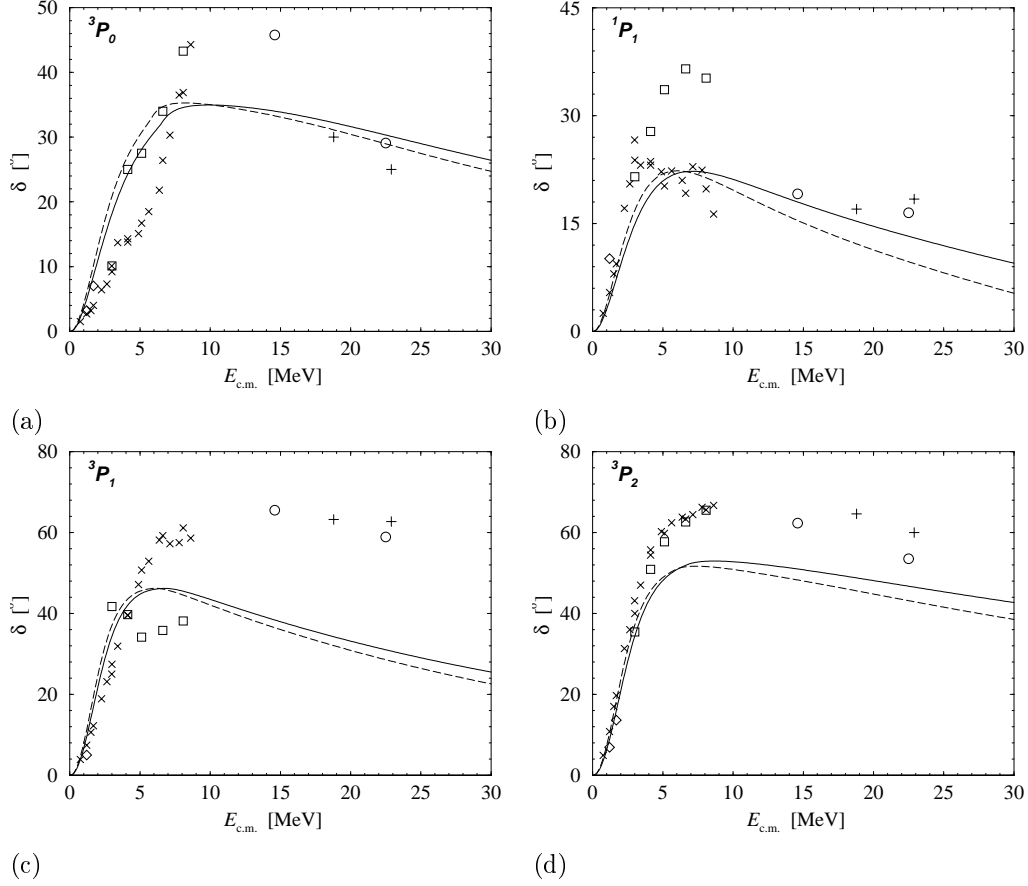


Fig. 3. The same as in figure 2 is shown but for the 3P_0 (a), 1P_1 (b), 3P_1 (c) and 3P_2 (d) phase-shifts.

4.3 Conclusions

We have discussed a new RRGm calculation of the ^4Li -scattering system using the Argonne- v_{14} - and the Bonn-interaction and two different model-spaces. The calculated phase-shifts have been compared to experimentally and theoretical obtained ones. The overall description of the phase-shifts is in very good agreement with the results of others [24,28,29,30,31]. Due to the fact that the Bonn-interaction is slightly more attractive than the Argonne- v_{14} -interaction leads to a better reproduction of the experimental data by the Bonn-potential. But the P -wave phase-shifts show not enough attraction. This result was also obtained by Pfitzinger et al. [27] and Viviani et al. [24]. Pfitzinger et al. and Viviani et al. have used the Argonne- v_{18} -interaction with three-particle-forces. At low energies the analyzing-power A_y can be reproduced by setting the 3P_2 phase-shift to the experimental determined one. Pfitzinger et al. [27] pointed out that also the 3P_0 phase-shift has to be corrected to get into agreement. Unfortunately our model-space is too small to make a statement to this result. But at higher energies it turns clearly out that not only the 3P_2 phase-shift

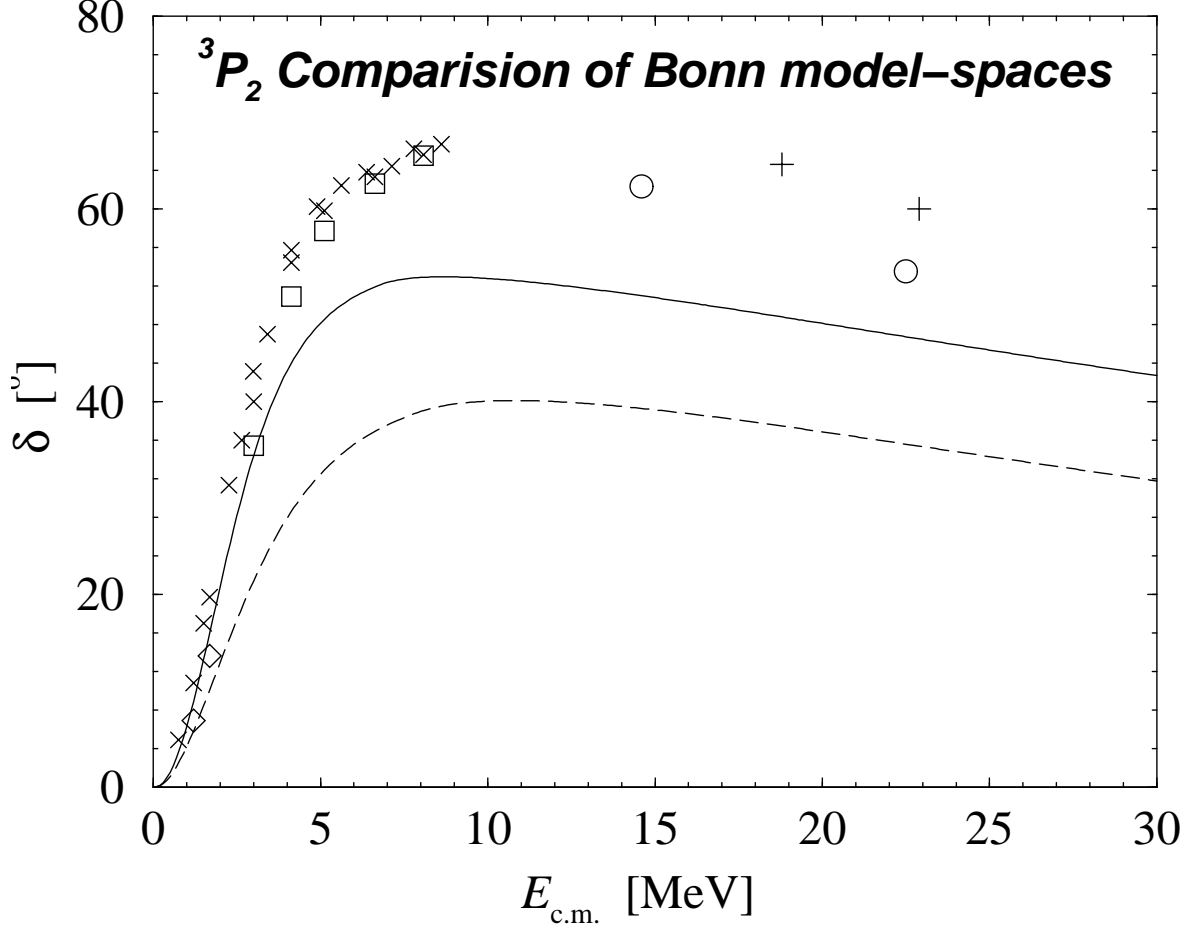


Fig. 4. The 3P_2 phase-shift is shown using the Bonn interaction for the medium (solid line) and the large model (dashed line) for the ^3He wave-function. For comparison results of other experimental and theoretical groups are shown as indicated in figure 2.

has to be corrected to reproduce analyzing-powers and cross-sections. And at low energies the contribution of three-particle-forces is negligible since we can reproduce all available phase-shifts within our model. The NN -interactions used yield large differences in the P -wave phase-shifts compared to experimental values. Pfitzinger et al. [27] have demonstrated that new contributions to the $3N$ -forces acting on P -waves should be considered especially for the description of the $^3P_2 - ^3P_0$ splitting. Therefore we consider this system well suited for further studies of the $3N$ -forces. All the realistic NN -interactions studied till now, av'_8 , av_{14} , av_{18} , and Bonn show the same behavior for all the P -wave phase shifts.

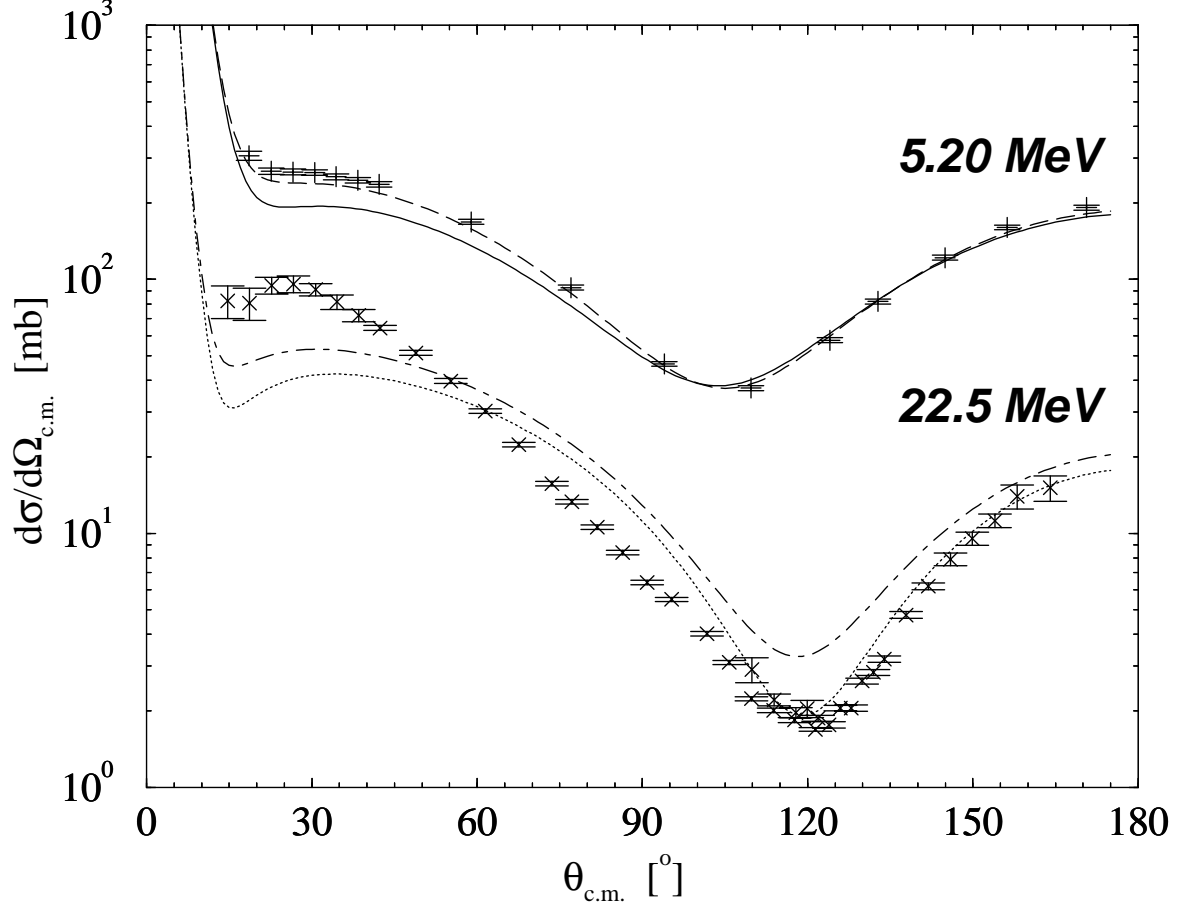


Fig. 5. The differential cross-section $d\sigma/d\Omega_{\text{c.m.}}$ in comparison with the experiments at $E_{\text{c.m.}} = 5.20$ MeV (solid line) and $E_{\text{c.m.}} = 22.5$ MeV (dotted dashed line) is shown. The curve where to the 3P_2 phase-shift 10.5° have been added at $E_{\text{c.m.}} = 5.20$ MeV is the dashed line. And the curve where to the 3P_2 phase-shift 15.0° have been added at $E_{\text{c.m.}} = 22.5$ MeV is the dotted line. The experimental data at $E_{\text{c.m.}} = 5.21$ MeV is taken from McDonald et al. [34] and at $E_{\text{c.m.}} = 23.0$ MeV from Harbison et al. [35].

Acknowledgments

The authors like to thank C. Winkler and J. Wurzer for fruitful discussions during this work. And in addition B. Pfitzinger not only for discussions but also for providing us with model-spaces for the fragments of the ${}^4\text{Li}$ -scattering-system. C.R. likes to thank W. Leidemann for discussions of the phase-shifts in the $(n - {}^3\text{He})$ scattering system.

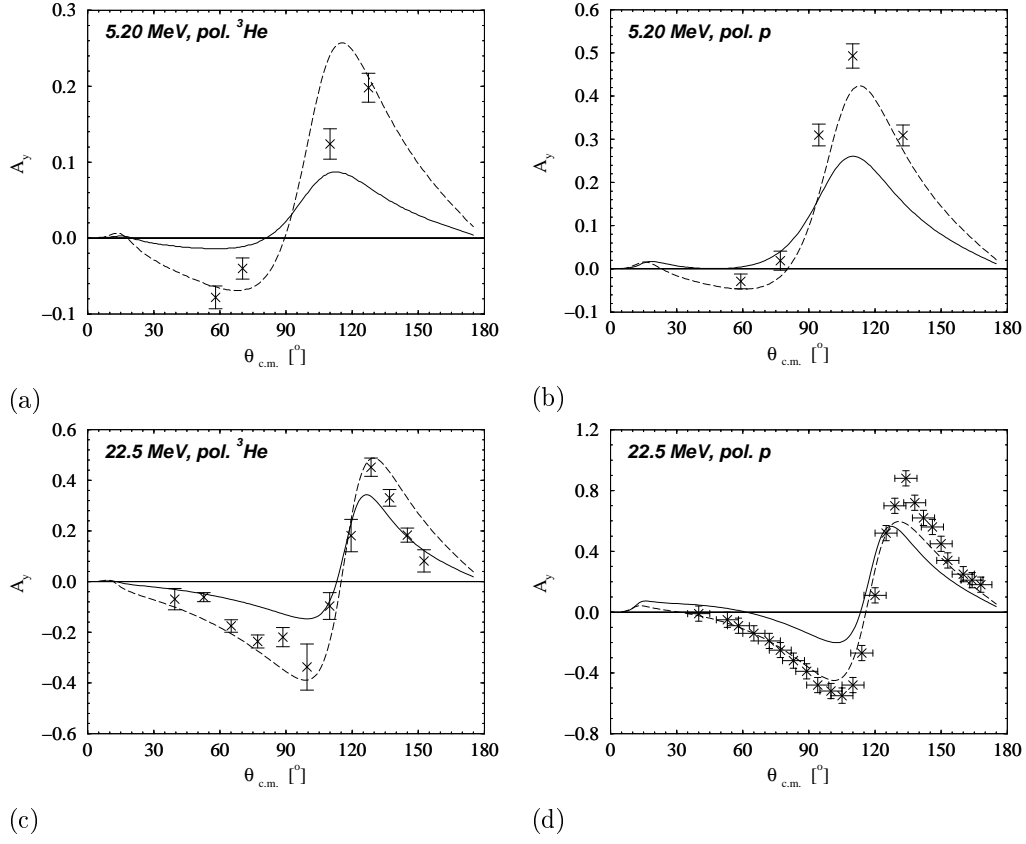


Fig. 6. The analyzing power A_y (solid line) is shown in comparison with experimental results (\times) with polarized ^3He at $E_{\text{c.m.}} = 5.20$ MeV and results of McSherry et al. [29] at $E_{\text{c.m.}} = 5.18$ MeV (a), with polarized protons at $E_{\text{c.m.}} = 5.20$ MeV and results of McDonald et al. [34] at $E_{\text{c.m.}} = 5.21$ MeV (b), with polarized ^3He at $E_{\text{c.m.}} = 22.5$ MeV and results of McCamis et al. [33] (c) and with polarized protons at $E_{\text{c.m.}} = 22.5$ MeV and results of Birchall et al. [32] (d). The curve where to the 3P_2 phase-shift 10.5° (subfigure (a) and (b)) and 15.0° (subfigure (c) and (d)) have been added to reach the experimental results is the dashed line.

References

- [1] H. Witala, D. Hüber and W. Glöckle, Phys. Rev. **C49** (1994) R14.
- [2] L.D. Knutson, L.O. Lamm and J.E. McAninch, Phys. Rev. Lett. **71** (1993) 3762.
- [3] A. Kievsky, S. Rosati, W. Tornow and M. Viviani, Nuc. Phys. **A607** (1996) 402.
- [4] A.Kievsky and W. Tornow, *Proton-Deuteron Phase-Shift Analysis above the Deuteron Breakup Threshold in TUNL Progress Report - XXXVIII*, TUNL, Durham, USA (1999).
- [5] H.M. Hofmann and G.M. Hale, Nucl. Phys. **A613** (1997) 69.

- [6] A.C. Fonseca, G. Hale and J. Haidenbauer, *Few-Body Systems* **31** (2002) 139.
- [7] R. Machleidt, F. Sammarruca and Y. Song, *Phys. Rev.* **C53** (1996) 1483.
- [8] V.G.J. Stokes, R.A.M. Klomp, C.P.F. Terheggen and J.J. de Swart, *Phys. Rev.* **C49** (1994) 2950.
- [9] R. Machleidt, *Adv. Nucl. Phys.* **19** (1989) 189.
- [10] D.R. Tilley, H.R. Weller, and G.M. Hale, *Nucl. Phys.* **A541** (1992) 1.
- [11] R.B. Wiringa, R.A. Smith und T.L. Ainsworth, *Phys. Rev.* **C 29** (1984) 1207.
- [12] H. Kellermann, H.M. Hofmann and Ch. Elster, *Few-Body Systems* **7** (1989) 31.
- [13] H.M. Hofmann, *Resonating Group Calculations in Light Nuclear Systems in Lecture Notes in Physics 273, Models and Methods in Few Body Physics*, Springer (1987).
- [14] R. Wölker, *Mikroskopische Analyse des 4-Helium-Systems im Hinblick auf die Möglichkeit eines neutronenfreien Fusionsreaktors*, Ph.D. thesis, Universität Erlangen-Nürnberg (1987).
- [15] W. Kohn, *Phys. Rev.* **74**, 1763 (1948).
- [16] A.R. Edmonds, *Angular Momentum in Quantum Mechanics*, Princeton University Press (1974).
- [17] C. Winkler and H.M. Hofmann, *Phys. Rev.* **C 55** (1997) 684.
- [18] G. Audi and A.H. Wapstra, *Nucl. Phys.* **A595** Vol.4 (1995) 405.
- [19] D.R. Tilley, H.R. Weller and H.H. Hasan, *Nucl. Phys.* **A474** (1987) 1.
- [20] I. Sick and D. Trautmann, *Nucl. Phys.* **A637** (1998) 559.
- [21] I. Reichstein, D.R. Thompson and Y.C. Tang, *Phys. Rev.* **C 3** (1971) 2139.
- [22] P. Heiss and H.H. Hackenbroich, *Nucl. Phys.* **A182** (1972) 522.
- [23] L. Beltramin, R. Del Frate and G. Pisent, *Nucl. Phys.* **A442** (1985) 266.
- [24] M. Viviani, A. Kievsky, S. Rosati, E.A. George and L.D. Knutson, *Phys. Rev. Lett.* **86** (2001) 3739.
- [25] R.B. Wiringa, V.G.J. Stokes and R. Schiavilla, *Phys. Rev.* **C 51** (1995) 38.
- [26] B.S. Pudliner et al., *Phys. Rev.* **C56** (1997) 1720.
- [27] B. Pfitzinger, H.M. Hofmann and G.M. Hale, *Phys. Rev.* **C64** (2001) 044003.
- [28] R. Darves-Blanc, Nguyen van Sen, J. Arvieux, J.C. Gondrand, A. Fiore und G. Perrin, *Nucl. Phys.* **A191** (1972) 353.
- [29] D.H. McSherry und S.D. Baker, *Phys. Rev.* **C1** (1970) 888.
- [30] D. Müller, R. Beckmann und U. Holm, *Nucl. Phys.* **A311** (1978) 1.

- [31] T.A. Tombrello, Phys. Rev. **B138** (1964) 40.
- [32] J. Birchall, W.T.H. van Oers, J.W. Watson, H.E. Conzette, R.M. Larimer, B. Leemann, E.J. Stephenson, P. von Rossen and R.E. Brown, Phys. Rev. **C 29** (1984) 2009.
- [33] R.H. McCamis, P.J.T. Verheijen, W.T.H. van Oers, P. Drakopoulos, C. Lapointe, G.R. Maughan, N.T. Okumusoglu and R.E. Brown, Phys. Rev. **C 31** (1985) 1651.
- [34] D.G. McDonald, W. Haeberli and L.W. Morrow, Phys. Rev. **133** (1964) B1178.
- [35] S.A. Harbison, R.J. Griffiths, N.M. Stewart, A.R. Johnston and G.T.A. Squier, Nucl. Phys. **A150** (1970) 570.